AFWAL-TR-84-4042

12

AD-A146 997

DESIGN AND TESTING OF A REFRACTIVE LASER BEAM HOMOGENIZER

Nils C. Fernelius
Kenneth R. Bradley, Capt., USAF
Brian L. Hoekstra, Lt., USAF

September 1984

Final Report for Period November 1982 - February 1984

20000802249

DTIC FILE COPY

MATERIALS LABORATORY
AIR FORCE WRIGHT AERONAUTICAL LABORATORIES
AIR FORCE SYSTEMS COMMAND
WRIGHT-PATTERSON AIR FORCE BASE, OHIO

NOTICE

When Government drawings, specifications, or other data are used for any purpose other than in connection with a definitely related Government procurement operation, the United States Government thereby incurs no responsibility nor any obligation whatsoever; and the fact that the government may have formulated, furnished, or in any way supplied the said drawings, specifications, or other data, is not to be regarded by implication or otherwise as in any manner licensing the holder or any other person or corporation, or conveying any rights or permission to manufacture use, or sell any patented invention that may in any way be related thereto.

This report has been reviewed by the Office of Public Affairs (ASD/PA) and is releasable to the National Technical Information Service (NTIS). At NTIS, it will be available to the general public, including foreign nations.

This technical report has been reviewed and is approved for publication.

BRIAN L. HOEKSTRA, 1LT., USAF
Laser & Optical Materials Branch

G. EDWARD KUHL, Chief
Laser & Optical Materials Branch
Electromagnetic Materials Division

FOR THE COMMANDER

MERRILL L. MINGES, Chief
Electromagnetic Materials Division
Materials Laboratory
Air Force Wright Aeronautical Laboratories

"If your address has changed, if you wish to be removed from our mailing list, or if the addressee is no longer employed by your organization please notify AFWAL/MLPO, W-PAFB, OH 45433 to help us maintain a current mailing list".

Copies of this report should not be returned unless return is required by security considerations, contractual obligations, or notice on a specific document.

Unclassified

SECURITY CLASSIFICATION OF THIS PAGE

REPORT DOCUMENTATION PAGE

1a. REPORT SECURITY CLASSIFICATION Unclassified	1b. RESTRICTIVE MARKINGS
2a. SECURITY CLASSIFICATION AUTHORITY	3. DISTRIBUTION/AVAILABILITY OF REPORT Approved for public release; distribution unlimited.
2b. DECLASSIFICATION/DOWNGRADING SCHEDULE	
4. PERFORMING ORGANIZATION REPORT NUMBER(S)	5. MONITORING ORGANIZATION REPORT NUMBER(S) AFWAL-TR-84-4042
6a. NAME OF PERFORMING ORGANIZATION Optical Laboratory Air Force Wright Aeronautical Laboratories/AFWAL	6b. OFFICE SYMBOL (If applicable) AFWAL/MLPO
6c. ADDRESS (City, State and ZIP Code) AFWAL/MLPO Wright-Patterson AFB, OH 45433	7a. NAME OF MONITORING ORGANIZATION
	7b. ADDRESS (City, State and ZIP Code)
8a. NAME OF FUNDING/SPONSORING ORGANIZATION	8b. OFFICE SYMBOL (If applicable)
8c. ADDRESS (City, State and ZIP Code)	9. PROCUREMENT INSTRUMENT IDENTIFICATION NUMBER
	10. SOURCE OF FUNDING NOS

PROGRAM ELEMENT NO	PROJECT NO	TASK NO	WORK UNIT NO
61102F	2306	23060	23060106

11. TITLE (Include Security Classification) Design and Testing of a Refractive Laser Beam Homogenizer

12. PERSONAL AUTHOR(S)
Sybil L. Cornelius, Capt Kenneth R. Bradley and Lt. Brian L. Hoekstra

13a. TYPE OF REPORT	13b. TIME COVERED	14. DATE OF REPORT (Yr., Mo., Day)	15. PAGE COUNT
Interim	FROM Nov 1982 TO Feb 1984	September 1984	43

16. SUPPLEMENTARY NOTATION

17. COSATI CODES			18. SUBJECT TERMS (Continue on reverse if necessary and identify by block number)
FIELD	GROUP	SUB. GR.	Laser Beam Homogenizer, Uniform Light Beam, Flat Top Laser Beam
20	06		
20	14		

19. ABSTRACT (Continue on reverse if necessary and identify by block number)

A survey is made of various techniques to create a homogeneous or flat top laser beam profile. A refractive homogenizer was designed for use with a ND:YAG laser with output at its fundamental (1.06 μm) and frequency doubled (532 nm) modes. The system consists of a 2X beam expander and two faceted cylindrical lenses with differing focal lengths. Each cylindrical lens focusses its input into a strip the width of 1 facet. By orienting their axes at a 90° angle and focussing them on the same plane, the beam is concentrated into a square focus. Formulae for calculating the facet angles are derived and a FORTRAN computer program was written to calculate them with a precision greater than one is able to fabricate them.

The nominal focal length of the lenses were run 15 cm and 20 cm. The focal spot was a 5 x 5 mm square. The lenses were fabricated for Corning 7940 Schlieren grade fused silica by Planar Optics, Inc. Webster, NY. They were then given a double V anti-reflective (AR)

20. DISTRIBUTION/AVAILABILITY OF ABSTRACT	21. ABSTRACT SECURITY CLASSIFICATION
UNCLASSIFIED/UNLIMITED ☒ SAME AS RPT ☐ DTIC USERS ☐	Unclassified

22a. NAME OF RESPONSIBLE INDIVIDUAL	22b. TELEPHONE NUMBER (Include Area Code)	22c. OFFICE SYMBOL
Lt. Brian Hoekstra	56671	AFWAL/MLPO

DD FORM 1473, 83 APR EDITION OF 1 JAN 73 IS OBSOLETE.

Unclassified

SECURITY CLASSIFICATION OF THIS PAGE

19. Abstract (Continued)

coating by CVI Laser Corporation, Albuquerque, NM. After fabrication, the system underwent several tests. The measured focal lengths were 15.4' cm and 20.75 cm measured roughly from the plane defined by the edge of the outer facet. Tests where a slit or pinhole passed across the focal square indicated a flat top profile within experimental limitations. A system consisting of a 2X beam expander plus the homogenizer had a throughput of 93% at 5[illegible] nm.

Next a silicon wafer was irradiated near damage threshold. Inspection of the damage region under a microscope revealed a rectangular array of damage spots with 15.6μm and 20.6μm spacings. A detailed theoretical analysis revealed that the spacing formula was similar to that encountered with a Young's double slit experiment. It predicts spacings of 16.0μm and 22.2μm. The surprising thing is that the spot patterns from various facets coincide. Thus, the refractive homogenizer must be used in conjunction with another device.

FOREWORD

This report describes an in-house effort conducted by personnel of the Laser and Optical Materials Branch (MLPO), Electromagnetic Materials Division (MLP), Materials Laboratory, Air Force Wright Aeronautical Laboratories (AFWAL), Wright-Patterson Air Force Base, Ohio under the Laser Annealing Project of Work Unit Directive 48.

The work reported herein was performed during the period November 1982 to February 1984 by Dr. Nils C. Fernelius (NRC Research Associate), Capt. Kenneth R. Bradley (AFWAL/MLPO) and Lt. Brian L. Hoekstra (AFWAL/MLPO). The report was released by the authors in February 1984.

The authors wish to thank the following for assistance in various aspects of this work. Mr. Timothy Peterson (AFWAL/MLPO) for insight in some of the calculations. Mr. Kenneth Beasley (AFWAL/MLPO) for assistance in the computer calculations. Mr. Gary Wolfe of Digital Optical Inc., Centerville, OH for suggesting Planar Optics as a fabricator. Dr. Patrick Hemenger (AFWAL/MLPO) for patience and encouragement during the many delays encountered. Mr. Curtis Atnipp (AFIT/EP) for experimental assistance in checking out the finished device using an argon laser. Mr. David V. Dempsey (UDRI) for making adjustable coaxial holders for the lenses in the X2 beam expander and for the faceted lenses. He also helped in the check-out work and was the first to observe the dot pattern of silicon surfaces at damage threshold.

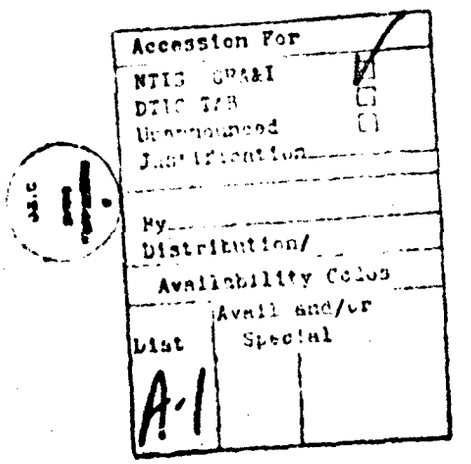

TABLE OF CONTENTS

LIST OF ILLUSTRATIONS

LIST OF TABLES

LIST OF SYMBOLS

w	The Width of the Desired Focal Square
θ	The Facet Angle Measured from the Direction of the Flat Face of the Lens
β	The Angle of the Emerging Light Beam Measured from the Normal to the Flat Face
h	The Distance from the Edge of the Center Facet to the Focal Point
m	An Index Standing for Which Facet Is Being Considered
n	The Index of Refraction of the Loss Material
$Ym = mW/h$	
θ'	The Value of θ Obtained Using the Rigorous and Not the Approximate Formula
f_0	Focal Lengths of a Lens
f_{eff}	$= f_0 + d(1 - 1/n)$ Effective Focal Length of a Lens Followed by a Slab of Glass of Thickness d and Index of Refraction n.
Δ	Optical Path Difference
y	Position on Axis Perpendicular to Direction of Laser Light Propagation

SECTION 1

INTRODUCTION

The output of high power lasers often has a varying spatial dependence. The output with a single TEMoo axial mode has a Gaussian dependence while often a uniform spatial ("flat top") dependence is desired. Ready (Reference 1) has summarized some early work along these lines. In laser annealing applications (References 2,3) it is also desirable to have some scrambling of the polarization of the beam to minimize the formation of surface ripple.

There has been a considerable amount of literature on the subject of shaping optical wavefronts for specific tasks. In addition to the uniform spatial intensity desired in many applications, the laser fusion program desires a beam which is a uniform spherically converging wavefront (Reference 4), and some high power lasers have an annular output from which a uniform circular cross-section front is desired (References 5,6). The rest of this discussion will concentrate on the production of a uniform wavefront from a point or disc source.

The production of a uniform wavefront can be achieved from a variety of methods. One commonly used technique is to divide a wavefront into segments and superimpose the image of each segment into one focal region. This approach divides into two general types, that of reflective optics and that of transmissive (refractive) optics. Another general type involves the use of special filtering devices. We shall proceed to enumerate examples from these three general areas.

The use of a segmented beam via reflective optics can take several forms. The Spawr Integrator (Reference 7) consists of a metal mirror consisting of a number of flat mirror segments approximating a concave mirror. The image of each segment is superimposed on the focal plane in space. With the capability of water cooling, very high powers can be handled. Somewhat more modest beam powers can be handled by a rectangular (References 9-11) or circular light pipe (References 11,12). An expanding beam traveling through a straight section produces images in a manner similar to a kaleidoscope. A circular light pipe with a 90° bend can also be used (Reference 12). Unless great care is taken, the above devices will lose more than half the power of the original beam.

There are several refractive techniques for homogenization which work best at not too high beam powers. One commonly used technique is to focus the beam with a short focal length lens onto a pinhole and create a spatial filter (Reference 13). A serious drawback to this technique is that a focused beam from even a moderately powered laser can cause breakdown in air. Also, it is difficult to find pinhole materials which would not be eroded away. By incorporating the device inside a vacuum system, somewhat higher powers can be handled at the expense of introducing additional optical surfaces and experimental complexity. A technique combining aspects of the kaleidoscope and spacial filtering methods is that of mirror folding of the beam (References 14-15). In this method a lens point focuses a beam at glancing incidents at the edge of a mirror. The resulting output can be focussed again at the edge of a second mirror. By this means parts of the incident beam are folded on top of each other. This can be repeated a number of times. Unfortunately, the point focus limits this to reasonably modest light powers. Another approach is to design beam expanders with aspheric lenses so that a Gaussian beam is transformed into a uniform plane wave front (References 16-20).

A refractive analog to Spawr's segmented mirrors was developed by Magee & McNab (Reference 21). In this case two faceted pieces similar to cylindrical lenses were fabricated with different focal lengths. The pieces are oriented with axes 90° with respect to each other and have a common focal point. Thus, the incoming beam results in a rectangle (or square) of superimposed images.

Uniformity through special filtering approaches can take several forms. Strictly speaking the spatial filter previously mentioned (Reference 13) should be included. Belvaux and Virdi (Reference 22) described a continuous tone filter generated simply by photographing the laser beam. They also mention that a binary filter could be used. Veldkamp (References 24-26) has described a number of systems using binary filters in both reflection and transmission modes.

SECTION II

DESIGN OF THE REFRACTIVE HOMOGENIZER

Following the work of Magee and McNab (Reference 21), we decided to construct an homogenizer which would give a flat top profile over a 0.5 cm square. The philosophy is to break up the laser beam with a faceted piece similar to a cylindrical lens. This device slices up the incoming beam into strips of width, W, and superimposes them (Figure 1). If a similar device with shorter focal length is positioned after this with axes at 90° to the first, thus, the strips are broken up and the final result is a square.

For purposes of calculation, it is easier to envision the flat face of the device facing the incoming beam. The diagram shown in Figure 2 shows the geometry of the system. θ is the facet angle measured from the direction of the flat face. ϕ is the angle of the emerging light beam measured from the normal to the flat face. For purposes of calculation we choose the midpoint of each facet and regard the light ray passing through it as passing through the focal point on the optic axis. The light rays passing through the upper and lower edges of the face would pass through points $\pm W/2$ off the optic axis. h is the distance from the central (zeroth) facet to the focal point.

As a first approximation, $\tan \phi_m = \frac{mW}{h}$ where (1)
$m = \pm 1, \pm 2, \pm 3, \ldots$ This ignores the small distance $\frac{W}{2} \tan \theta_m$ added at each facet face. Including this effect, we obtain a more complicated formula. The rigorous formula is

$$\tan \phi_m = \frac{mW}{h + \frac{W}{2} \tan \theta_m + W \sum_{i=1}^{m-1} \tan \theta_i} \quad (2)$$

Using Snell's law and the geometry shown in Figure 3, we have (assuming that n=1 for air), $n \sin \theta_m = \sin (\theta_m + \phi_m) = \sin \theta_m \cos \phi_m + \sin \phi_m \cos \theta_m$ so $n \tan \theta_m = \tan \theta_m \cos \phi_m + \sin \phi_m$

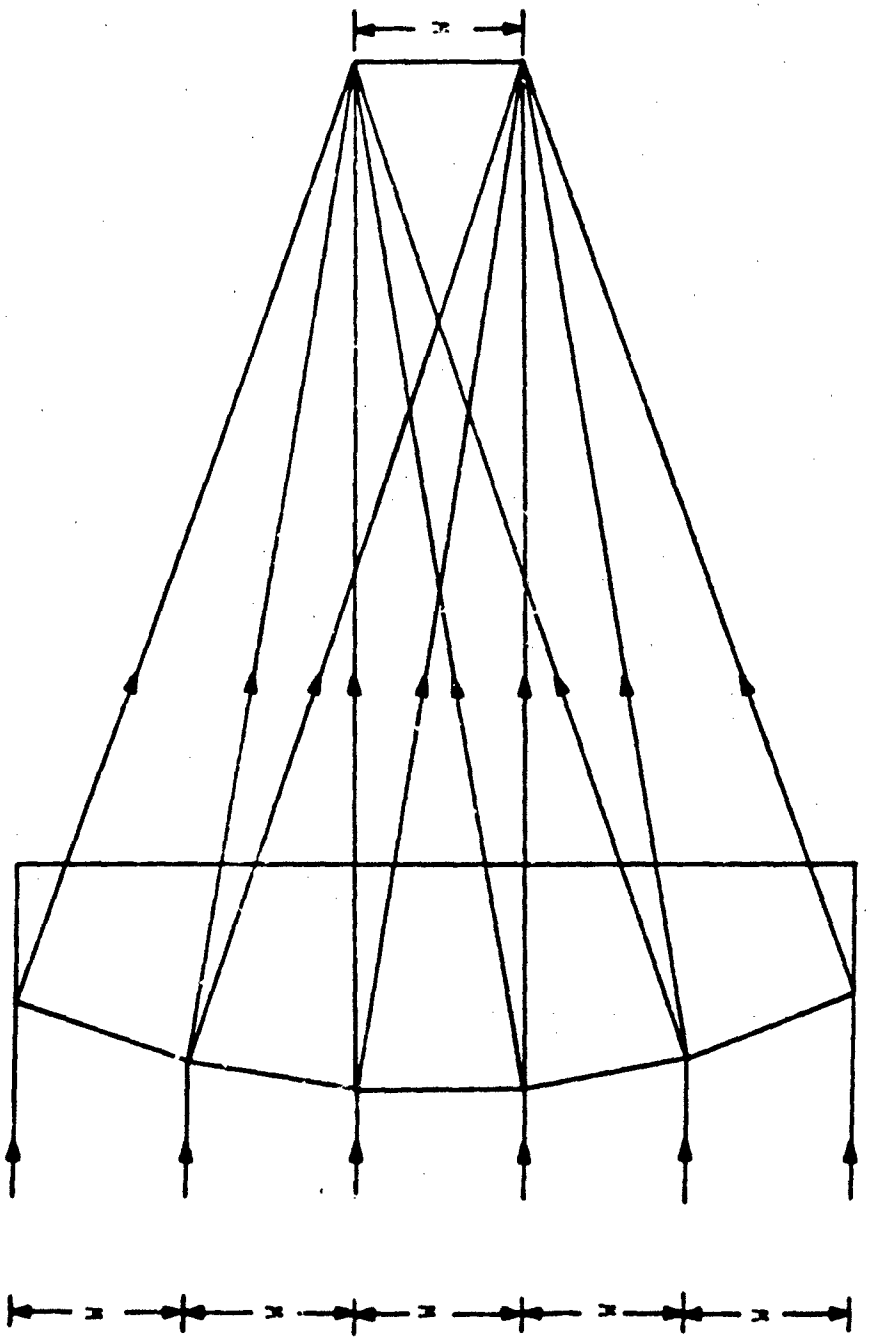

Figure 1. Diagram of Light Paths Through a Faceted Lens

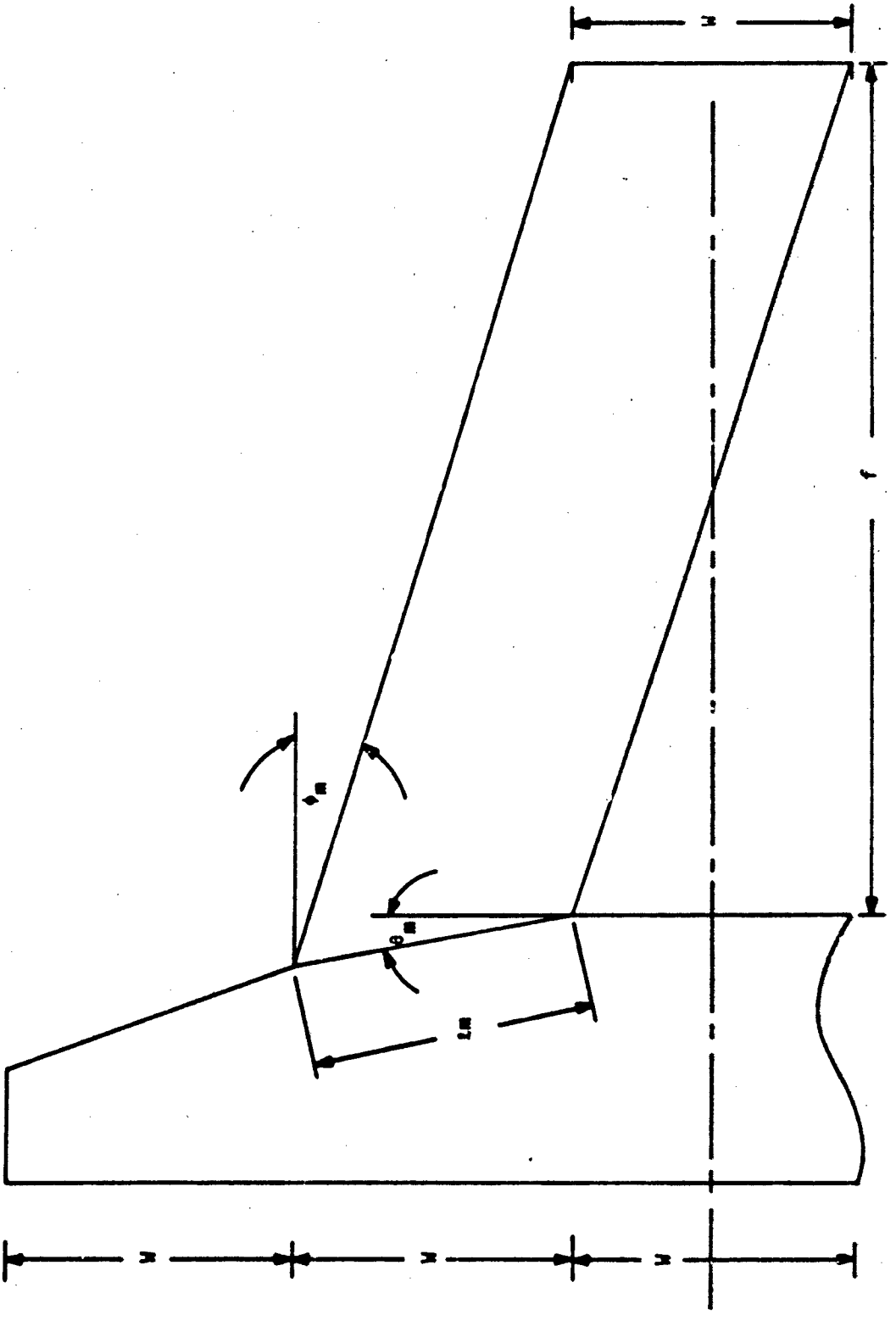

Figure 2. Diagram of the Light Paths Through the m^{th} Facet of a Faceted Lens

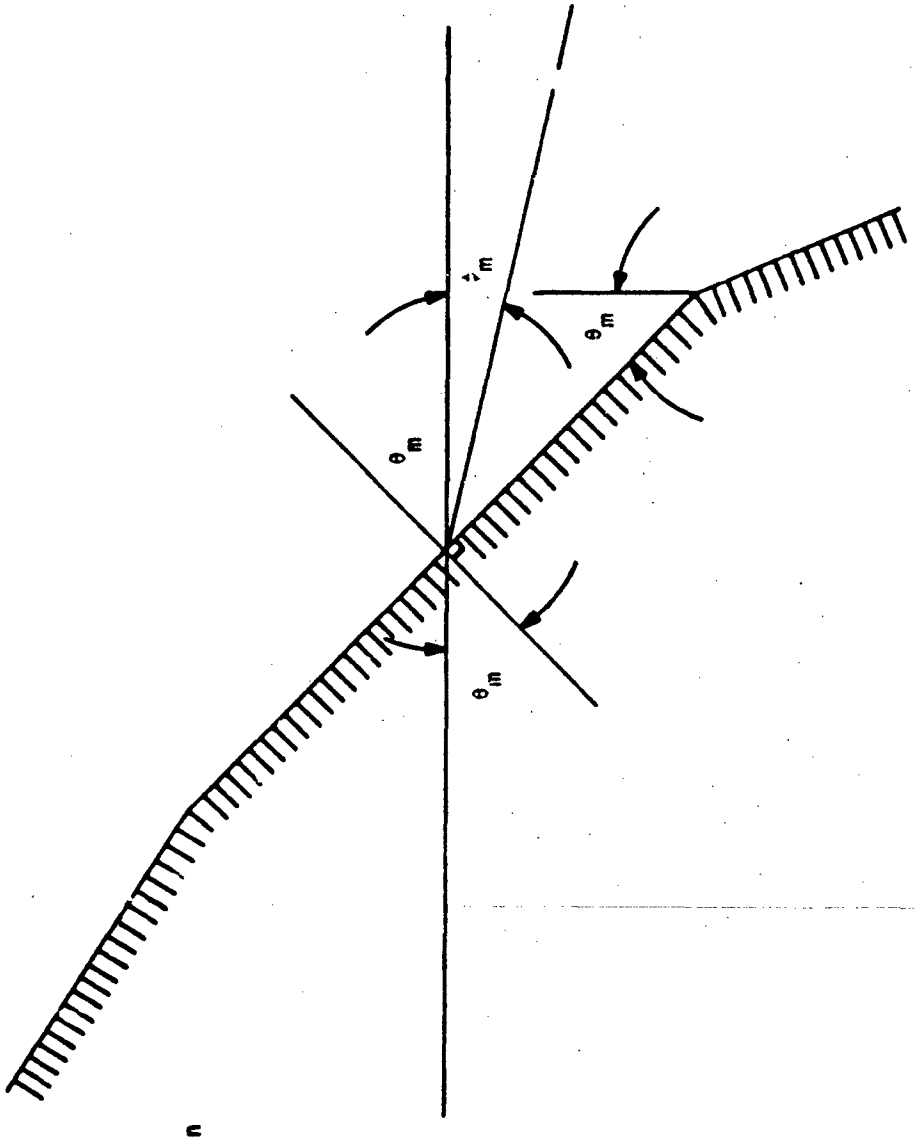

Figure 3. Detailed Drawing of the Angles Occurring for a Light Beam Passing Through the Center of a Facet

or

$$\tan \phi_m = \left\{ \frac{n}{\cos \phi_m} - 1 \right\} \tan \theta_m$$

$$= \left\{ n\sqrt{1 + \tan^2 \phi_m} - 1 \right\} \tan \theta_m \qquad (3)$$

Defining

$$y_m \equiv mW/h \qquad (4)$$

We have for the approximate formula

$$\tan \theta_m = \frac{y_m}{n\sqrt{1 + y_m^2} - 1} \qquad (5)$$

$$\theta_m = \arctan \left\{ \frac{y_m}{n\sqrt{1 + y_m^2} - 1} \right\} \qquad (6)$$

Let the rigorous value of θ_m be ψ_m. Then

$$\tan \psi_m \left[n\sqrt{1 + y_m^2} - 1 \right] = \frac{y_m}{1 + \frac{W}{2h} \tan \theta_m + \frac{W}{h} \sum_{i=1}^{m-1} \tan \psi_i}$$

or

for $m \geq 2$

$$\psi_m = \arctan \left\{ \frac{y_m}{\left[n\sqrt{1+y_m^2} - 1\right]\left[1 + \frac{y_1}{2} \tan \psi_m + y_1 \sum_{i=1}^{m-1} \tan \psi_i\right]} \right\} \qquad (7)$$

when $m = 1$

$$\psi_1 = \arctan \left\{ \frac{y_1}{\left[n\sqrt{1+y_1^2} - 1\right]\left[1 + \frac{y_1}{2} \tan \psi_1\right]} \right\} \qquad (8)$$

Since the correction terms are small, we replace ψ_m by θ_m in the denominator of the argument in Equation 7. A FORTRAN program has been written to calculate

$$\psi_m = \arctan\left\{\frac{y_m}{[n\sqrt{1+y_m^2}-1][1+\frac{y_1}{2}\tan\theta_n + y_1\sum_{i=1}^{m-1}\tan\psi_i]}\right\} \tag{9}$$

and

$$\psi_1 = \arctan\left\{\frac{y_1}{[n\sqrt{1+y_1^2}-1][1+\frac{y_1}{2}\tan\theta_n + y_1\sum_{i=1}^{m-1}\tan\psi_i]}\right\}$$

$$= \arctan\left\{\frac{y_1}{\frac{y_1^2}{2} + n\sqrt{1+y_1^2}=1}\right\} \tag{10}$$

We are mainly interested in a laser beam homogenizer for 532 nm, however, it should also operate at 1.06 μm wavelength. Heraeus Amersil makes a variety of fused silicas. However, the same index of refraction is quoted for all synthetic fused quartz.

TABLE 1

TABLE OF REFRACTIVE INDEX OF HERAEUS AMERSIL FUSED SILICAS FOR VARIOUS WAVELENGTHS

Wavelength, λ	Refractive Index at 20°C
486.13 nm	1.46314
546.07 nm	1.46007
1.00 μm	1.450473
1.10 μm	1.449261

Corning Glass Works makes a premium quality fused silica material (Code 7940). It quotes refractive index values for it at 20°C.

TABLE 2

TABLE OF REFRACTIVE INDEX OF CORNING GLASS WORKS FUSED SILICA CODE 7940 FOR VARIOUS WAVELENGTHS

λ in μm	n
0.5	1.46233
0.55	1.45991
1.0	1.45042
1.3	1.44692

As a compromise between values at the two wavelengths, we calculated the facet angles for n = 1.455. Calculations were also made for n = 1.460 and n = 1.450. The calculations were made for a focal square with 0.5 cm sides and for focal lengths of 15 and 20 cm. The results are given in Tables 3 and 4. For a 15 cm focal length the facet angles decreased with increasing n. For the first facet angle the values obtained are 4.224°, 4.178°, and 4.132° respectively; for the fifth facet 19.000°, 18.817°, and 18.637°. For the 20 cm focal length lens the values for the first facet are 3.174°, 3.140° and 3.106°; for the fifth facet, 14.919°, 14.768° and 14.619°.

After much searching we found a company capable of grinding and polishing such a device. The name of the company was: Planar Optics, Inc., 858 Hard Road, Webster, NY 14580, Phone (716) 671-0100.

Figures 4, 5 and 6 include some of the information included with the purchase order. The pieces were fabricated from Corning 7940 Scullieren grade fused silica. Figure 7 shows the lenses as received from Planar Optics. The coin is a half dollar. Figure 8 depicts the lenses in the same configuration in which they are used in the system.

Since the device will be used in an ND:YAG laser annealing facility, where fundamental (1.06 microns) and doubled (532 nm) light will impinge on the sample, a double V antireflective (AR) coating was applied to both surfaces of each lens. The vendor for this service was: CVI Laser Corporation, 200 Dorado Place, SE, P.O. Box 11308, Albuquerque, NM 87192, Phone (505) 296-9541.

TABLE 3

OUTPUT OF COMPUTER PROGRAM FOR FOCAL LENGTH 15 CM AND 0.5 CM WIDTH OF FOCAL SQUARE USING THREE INDICES OF REFRACTION

FOCAL LENGTH	WIDTH OF FOCAL SQUARE
15.000	0.500

INDEX OF REFRACTION
1.4500

FACET	PI IN DEGREES	THETA	LENGTH
1	4.22367	4.22886	0.5014
2	8.32764	8.36798	0.5053
3	12.20674	12.33676	0.5116
4	15.78093	16.07071	0.5196
5	19.99962	19.52498	0.5288
6	21.84022	22.67441	0.5387
7	24.30304	25.51113	0.5486
8	26.40461	28.04065	0.5582
9	28.17163	30.27786	0.5672
10	29.63600	32.24351	0.5753

INDEX OF REFRACTION
1.4550

FACET	PI IN DEGREES	THETA	LENGTH
1	4.17753	4.18261	0.5013
2	8.23826	8.27774	0.5052
3	12.07935	12.20669	0.5113
4	15.62219	15.90626	0.5192
5	18.81665	19.33217	0.5282
6	21.63986	22.45929	0.5379
7	24.09131	25.27925	0.5477
8	26.18654	27.79690	0.5572
9	27.95119	30.02631	0.5660
10	29.41623	31.98746	0.5740

INDEX OF REFRACTION
1.4600

FACET	PI IN DEGREES	THETA	LENGTH
1	4.13239	4.13736	0.5013
2	8.15077	8.18942	0.5051
3	11.95456	12.07931	0.5111
4	15.46654	15.74506	0.5188
5	18.63707	19.14301	0.5277
6	21.44299	22.24800	0.5372
7	23.88304	25.05129	0.5468
8	25.97180	27.55703	0.5562
9	27.73392	29.77856	0.5649
10	29.19940	31.73505	0.5728

TABLE 4

OUTPUT OF COMPUTER PROGRAM FOR 20 CM FOCAL LENGTH OF FOCAL SQUARE USING THREE INDICES OF REFRACTION

FOCAL LENGTH	WIDTH OF FOCAL SQUARE
20.000	0.500

INDEX OF REFRACTION
1.4500

FACET	PI IN DEGREES	THETA	LENGTH
1	3.17444	3.17664	0.5008
2	6.29768	6.31498	0.5030
3	9.32211	9.37898	0.5067
4	12.20678	12.33676	0.5116
5	14.91936	15.16205	0.5174
6	17.43700	17.83482	0.5241
7	19.74607	20.34150	0.5312
8	21.84109	22.67441	0.5387
9	23.72339	24.83117	0.5462
10	25.39937	26.81353	0.5535

INDEX OF REFRACTION
1.4550

FACET	PI IN DEGREES	THETA	LENGTH
1	3.13968	3.14183	0 5008
2	6.22940	6.24633	0.5030
3	9.22267	9.27833	0.5065
4	12.07938	12.20669	0.5113
5	14.76779	15.00564	0.5171
6	17.26525	17.65543	0.5236
7	19.55813	20.14256	0.5306
8	21.64071	22.45929	0.5379
9	23.51397	24.60299	0.5453
10	25.18386	26.57516	0.5525

INDEX OF REFRACTION
1.4600

FACET	PI IN DEGREES	THETA	LENGTH
1	3.10566	3.10777	0.5007
2	6.16257	6.17914	0.5029
3	9.12531	9.17981	0.5064
4	11.95459	12.07931	0.5111
5	14.61920	14.85235	0.5167
6	17.09676	17.47950	0.5231
7	19.37360	19.94733	0.5300
8	21.44380	22.24800	0.5372
9	23.30800	24.37872	0.5444
10	24.97176	26.34070	0.5516

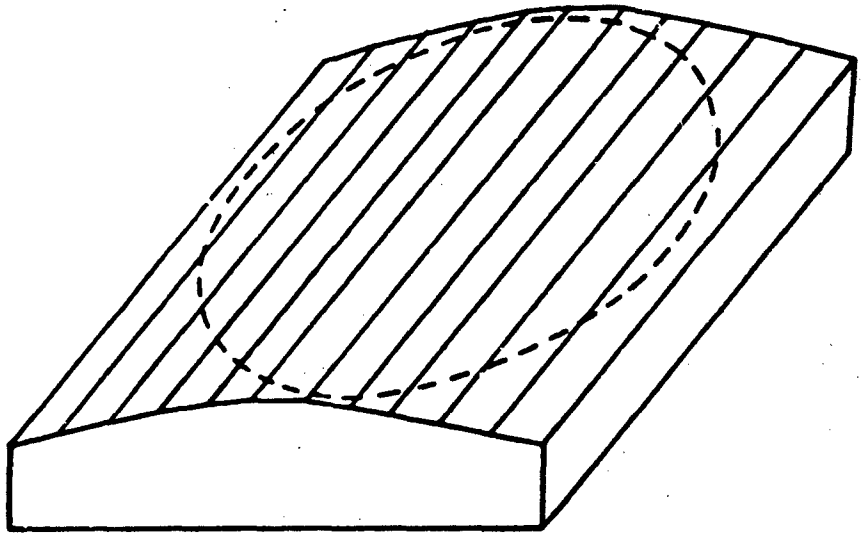

Figure 4. Angle Drawing of a Faceted Lens

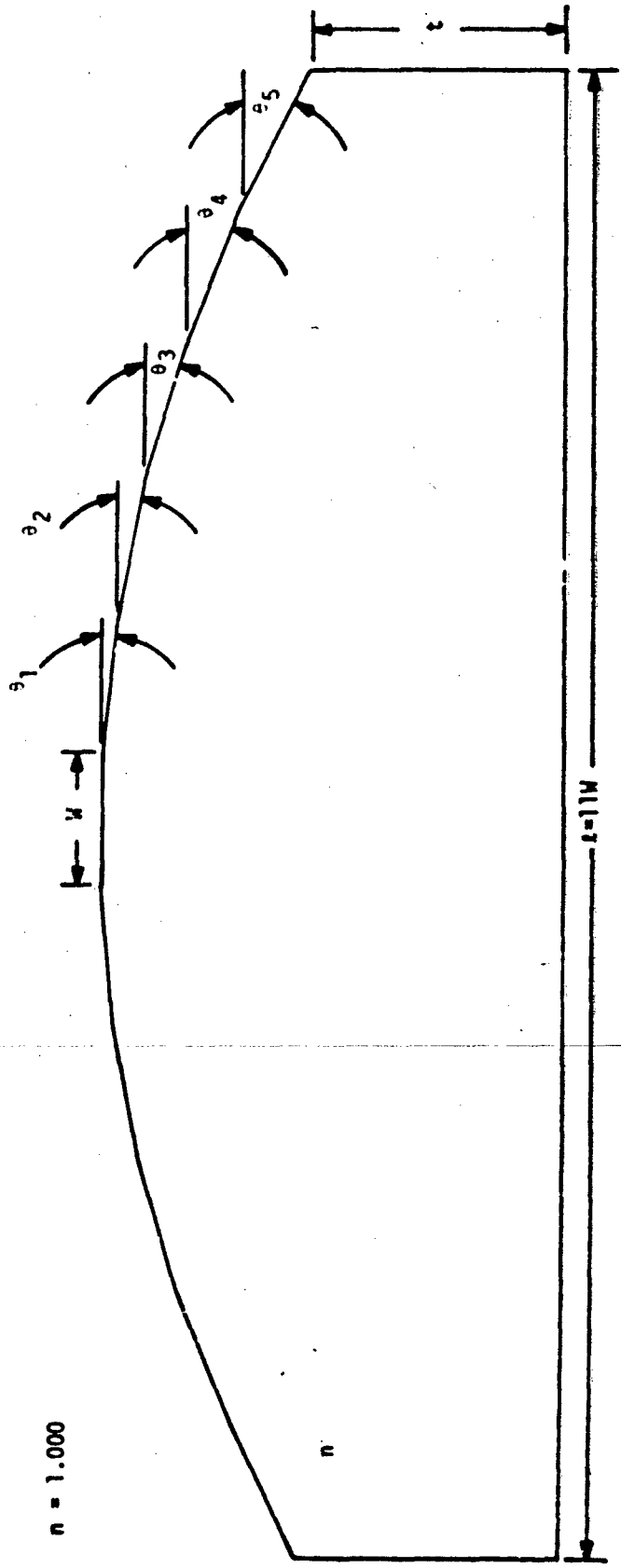

Figure 5. Cross-Sectional Drawing of a Faceted Lens

LASER BEAM HOMOGENIZERS REVISED

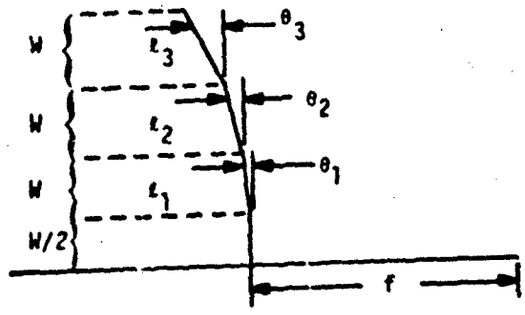

n = 1.455
W = 0.50 cm
f = 15, 20 cm

	f = 15 cm			f = 20 cm	
facet	θ_n	facet width ℓ_n	facet	θ_n	ℓ_n
0	0°	0.500 cm	0	0°	0.500 cm
1	4.18°	0.501	1	3.14°	0.501
2	8.24°	0.505	2	6.23°	0.503
3	12.08°	0.511	3	9.22°	0.507
4	15.62°	0.519	4	12.08°	0.511
5	18.82°	0.528	5	14.77°	0.517

Figure 6. Copy of Specifications Sheet Furnished to Fabricator

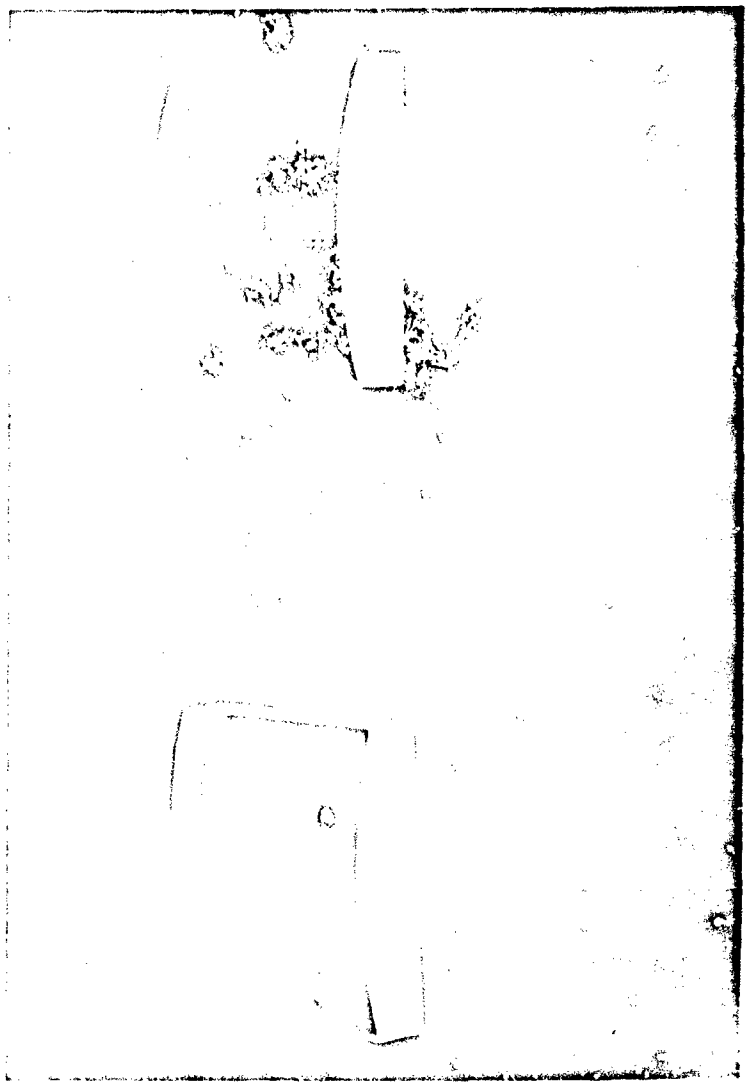

Figure 7. Photograph of a Faceted Lenses when Received from Planar Optics. The Coin is a half dollar

Figure 8. Photograph of Faceted Lenses in the Same Configuration in Which They Will Be Used

SECTION III

TESTING OF THE REFRACTIVE HOMOGENIZER

Initial tests on the faceted lenses were performed in the Air Force Institute of Technology (AFIT) student laboratories between semesters. An air-cooled Argon Laser Spectra Physics Model 162 was used for the light source. It was tuned to the 514.5 nm green line. A Jodon LP SF-100 spatial filter with EET-25 laser collimator was used to expand the beam. Then the 2X laser beam expander was put in line. Still further magnification was desired so further expansion was achieved with a negative and positive lens system. The resulting beam was checked to ensure that it was collimated over the length of the optical bench. Subsequent results indicate that it was still slightly diverging.

Over a month later the focal length tests were repeated using a Spectra Physics 155 Helium-Neon laser with about 3/4 milli-watt output at 633 nm. This beam was expanded with a Tropel Model 261 spatial filter and collimator. Initial test on the h=15 cm lens with the flat face towards the incident beam yielded a line focus strip 16.4 + 0.1 cm from the flat face. Reversing the lens so that the faceted side faced the beam yielded a focal strip 14.5 cm from the flat face. This lens was 1.4 cm thick at the central facet and about 0.9 cm at the edges. Assuming reciprocity is valid, the focal length of the lens should be the average of these, viz. 15.45 cm. This indicates that the optical center is 0.95 cm in from the flat face or about the plane defined by the outer edge of the last facet. Initial measurements with the argon laser yielded a focal length of 15.8 cm.

The lenses with h=20 cm underwent similar tests. The lens was 1.3 cm thick at the central facet, at the edges about 0.9 cm. The focal strip was 19.8 cm from the flat face with the light incident on the faceted face; 21.7 cm, on the flat face. The average focal length is 20.75 cm measured 0.95 cm in from the flat face. Preliminary results using the argon laser had yielded 22.65 cm.

In operation, light hits the "20 cm" lens first and then the "15 cm" lens oriented at a 90° angle. Even though the second lens only focuses light in the direction ignored by the first lens, its thickness does affect the effective focal length of the first lens. A slab of glass of thickness d and index of refraction, n, placed between

a lens and its focal spot, yields an effective focal length $f_{eff} = f_o + f(1 - 1/n)$. For the central facet we have $f_{eff} = 20.75$ cm + 1.4 cm (1 -1/1.455) = 20.75 + 1.4 (0.3127).
= 20.75 + 0.44 = 21.19 cm.

Thus, to focus on the same plane, the separation of the flat faces of the two lenses should be 5.74 cm.

The next experiment at AFIT was to sweep a slit across the focal plane of the crossed lenses (flat faces 6.7 cm apart) with a photomultiplier tube behind it. The slit width was 145 μm. The photomultiplier was an American Instrument Company, Model 10-213. Sweeps were made on two consecutive days. A steep rise in signal intensity was observed on entering the illuminated region. A fairly flat signal was then observed with a sharp rise occurring at trailing edge just before dropping to the background level. This occurred on sweeps going in different directions. These spikes are an indication that the photomultiplier was saturated. The half intensity points were separated by 5.7 mm. Plots of signal readings versus slit position are shown in Figures 9 and 10.

This type of experiment was repeated when we returned to the laser annealing apparatus. A hole about 0.8 mm in diameter was drilled in a thin brass plate. This was placed over the entrance hole of a Scientech 832 power head. The power head was mounted on the programmable x-y table. The resulting signal after the detecting equipment had reached steady state (usually after 3-5 pulses on at 1 Hz rep rate) was read on a Scientech 362 power energy meter on the 0.003 watt scale. The x-y table was programmed to move in steps of 0.162 mm. Figure 11 shows a plot of resulting signal versus number of steps. It is evident that the brass plate heated up during the experiment reradiating into the power meter, since the original base line was not reached after passing through the square. The separation between the half amplitude points is 4.7 mm.

Figure 12 shows burn patterns of the doubled YAG beam taken at various locations in the laser annealing facility. The burn patterns indicate a cross section of the energy profile of the laser beam. Before and after the 2X laser beam expander, the beam has a number of inhomogeneities. Diffraction effects due to the coherence of the TEM_{00} mode are the cause of most of these effects. The square focus region is much more intense and uniform indicating considerable improvement in the beam.

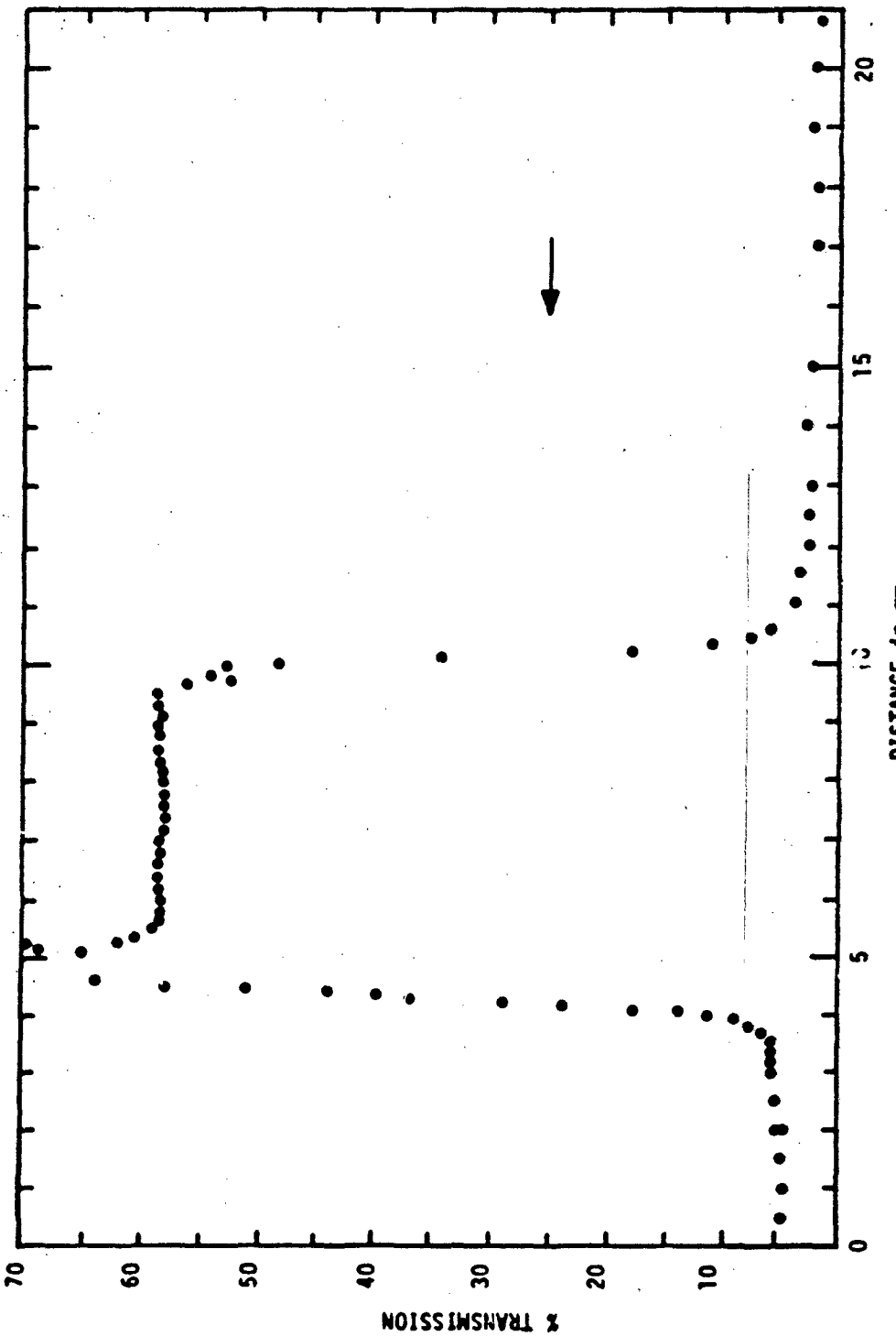

Figure 9. Photomultiplier Signal Reading versus Entrance Slit Position in Focal Plane of Faceted Lenses. First Run

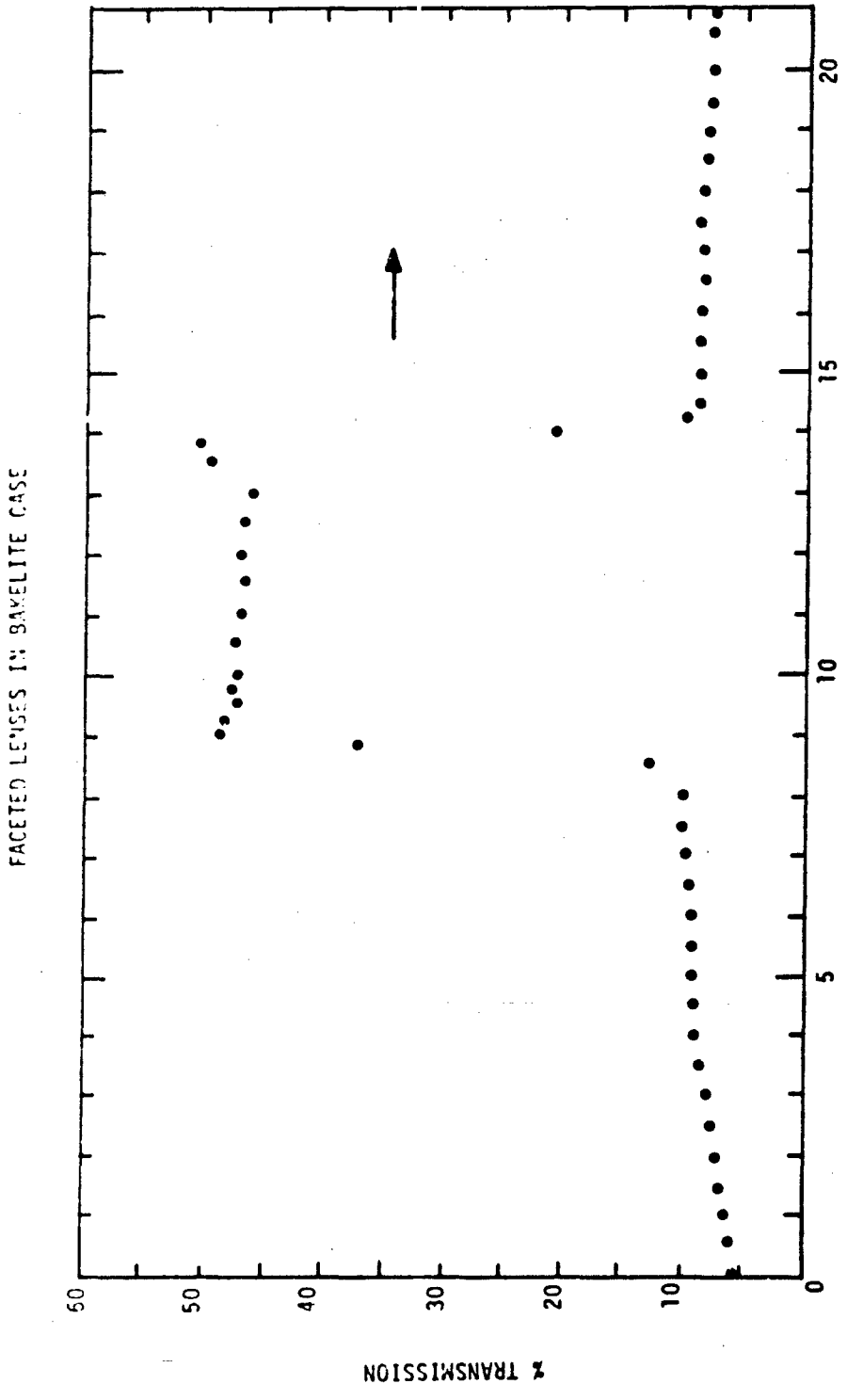

Figure 10. Photomultiplier Signal Readings versus Entrance Slit Position in Focal Plane of Faceted Lenses. Second Run

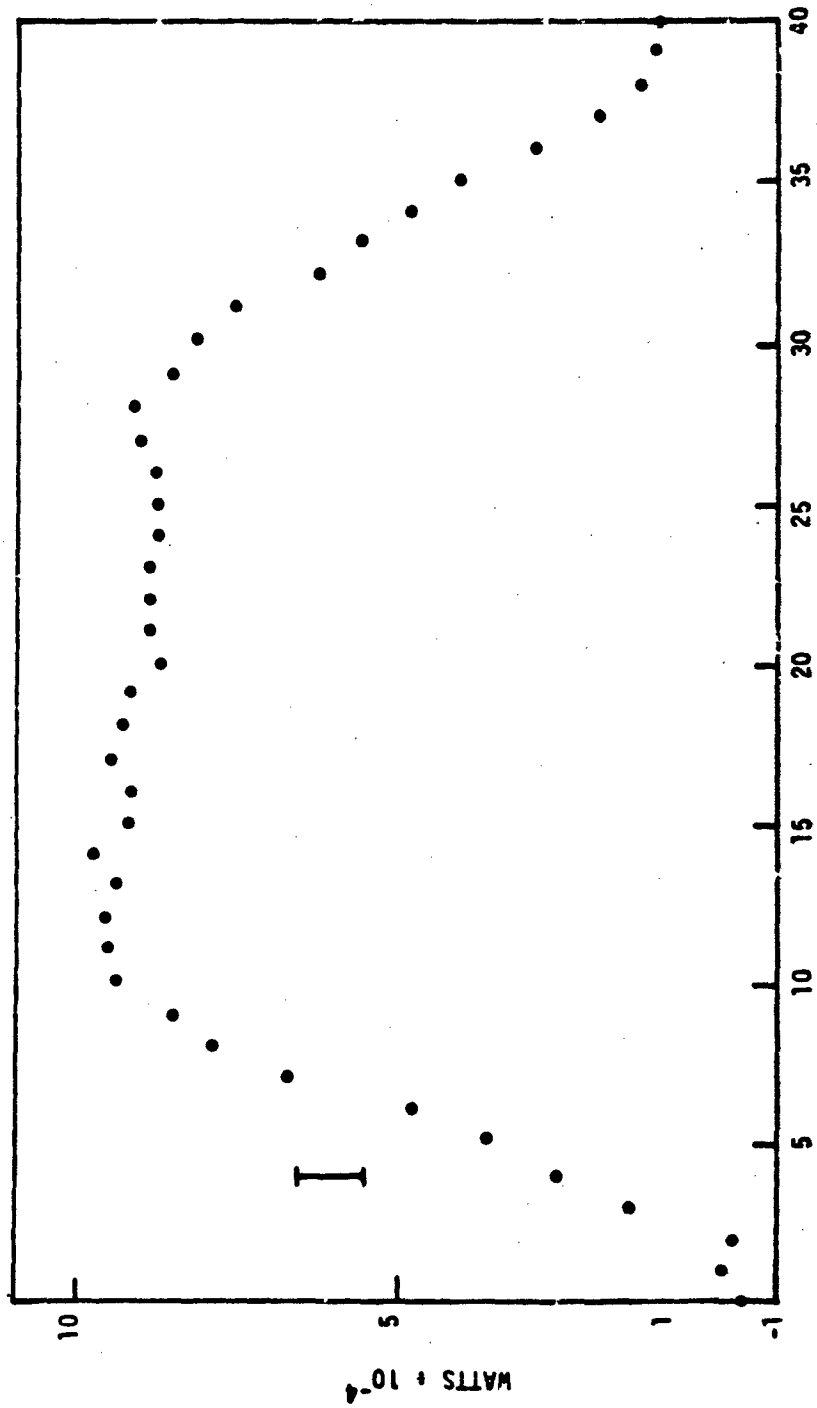

Figure 11. Power Meter Readings versus Number of Steps Taken on x-y Table

Figure 12. Photograph of Burn Patterns on Photosensitive Paper Showing Cross Sections of Laser Beam at Various Positions in the Annealing Facility

With a 532 nm beam, the power was measured before entering the 2X beam expander. The power out of the beam expander and faceted lenses combination was measured to be 93 of the input to the system.

Next some experiments were performed to determine the threshold at 532 nm for damage on the surface of a silicon wafer. When a damaged region was observed, it was inspected under a microscope. An unexpected regular array of damage spots was observed. Figure 13 shows a picture of the damaged region with energy density of about $2J/cm^2$ under 65X magnification. Figure 14 shows about $1/2\ J/cm^2$ under 65X magnification. Figure 15 shows a photograph of about $1/2\ J/cm^2$ at 520 X magnification. The separation of dots in one direction is about 1.9 cm; in the other direction 1.5 cm. As a check on accuracy, measurements were made over four spacings yielding 7.8/4 = 1.95 cm average separation in one direction; in the other direction the measurement was 5.9/4 = 1.475 cm. The ratio of these is 1.322. As an additional check, measurements were made on the 65X magnification picture. Averaging over 20 spacings, 4.7 cm/20 = 2.35 mm (0.235 x 520/65 = 1.88 cm) in one direction; 6.0 cm/33 = 1.818 mm (0.1818 x 520/65 = 1.4545 cm) in the other direction. This ratio is 1.293, thus the two scales are rougly equivalent. To calibrate the microscope, a reticule with lines 100 μm apart was laid over the sample on a 65X scale. A 300 μm separation was 35.5 mm apart, thus 1 mm = 8.4507 μm on the 65X scale. Measurements on the dot pattern below the reticule were 1.909 mm and 2.444 mm with a ratio 1.2803. In the real world, these spacings are 16.13 μm and 20.65 μm. The earlier results at 65X are 15.36 μm and 19.86 μm. For the 520X pictures the scale factor is 1 cm = 10.563 μm, so the spacings are 15.58 μm and 20.60 μm.

Another test was made with a pure 1.06 μm beam of about $2J/cm^2$ energy density. Figure 16 shows the resulting pattern. The oval damage patterns made it a bit difficult to measure their centers. The measured spacings were 3.2 cm and 4.1 cm or 33.80 μm and 43.31 μm. The ratio of these numbers is 1.281. These numbers are a bit larger than twice those measured at 532 nm although their ratios are almost identical. Perhaps a slightly different focal plane position was used in the two shots. However, this experiment is rather conclusive proof that the spacing varies linearly with laser wavelength.

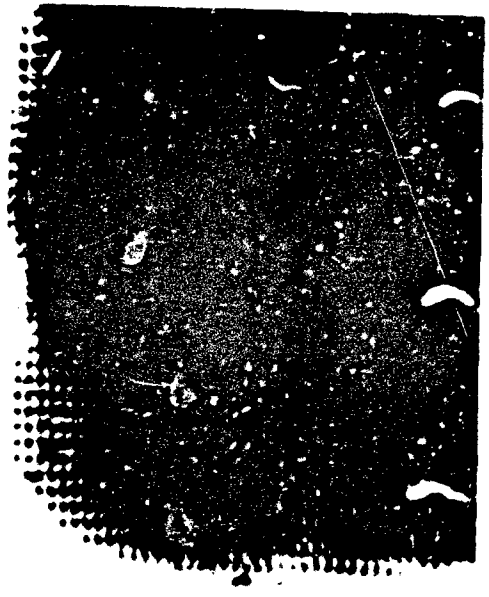

Figure 13. Damage Regions on Silicon Wafer with about 2J/cm^2 Input Energy Density at 532 nm. Nominal Mag. 65X

Figure 14. Damage Regions on a Silicon Wafer with about 1/2 J/cm^2 Input Energy Density at 532 nm. Nominal Mag 65X

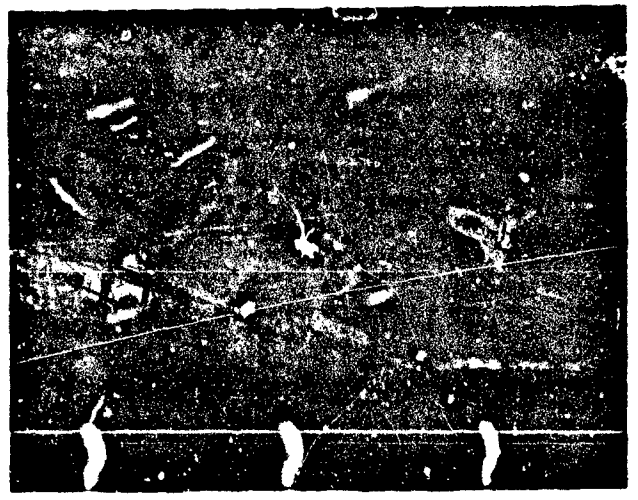

Figure 16. Damage Regions on a Silicon Wafer with about 1/2 J/cm^2 Input Energy at 1.06 Microns. Nominal Mag 520X

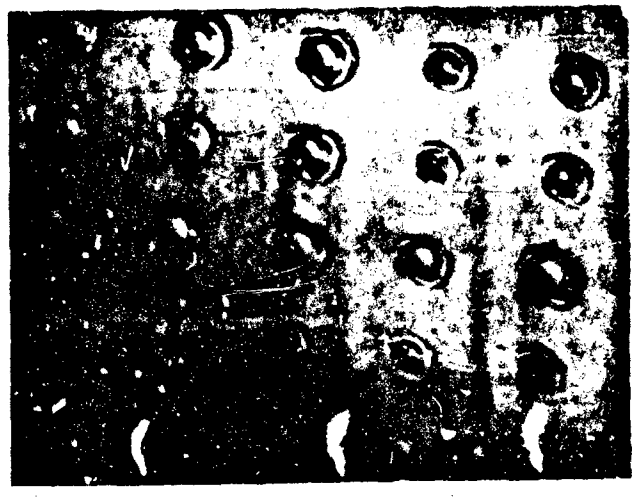

Figure 15. Damage Regions on a Silicon Wafer with about 1/2 J/cm^2 Input Energy Density at 532 nm. Nominal Mag 520X

Since the laser has a fairly long coherence length, we have a situation analogous to the Young double and multiple slit experiments for light coming from the facets. However, there is a slight difference since some of the light from planes of equal phase passes through the lens material instead of air. For simplicity a detailed analysis will be done for the central facet and one adjacent one. Figure 17 describes the situation. We shall regard the collimated beam as a plane wavefront. The first facet folds a wavefront of width W onto the undeflected part of the beam going through the central facet also of width W. At the top of the first facet the optical path to the image is $\sqrt{W^2 + (h + W \tan \theta_1)^2}$. The optical path for light passing through the top of the central facet is $(n W \tan \theta_1 + h)$. Measuring the distance y from the top of each facet we have in general for the optical path for a wavefront intersecting the first facet a distance y down from the top

$$\sqrt{W^2 + [h + (W-y)\tan \theta_1]^2}$$

The optical path for a beam through the central facet is

$$n(W-y) \tan \theta_1 + h$$

The optical path difference, Δ, is $\Delta = n (W-y) \tan \theta_1 + h - \sqrt{W^2 + [h + (W-y) \tan \theta_1]^2}$.

In our system W = 0.5 cm and h-15-20 cm, thus we can write

$$\Delta = [h + n(W-y) \tan \theta_1] - [h + (W-y) \tan \theta_1] \sqrt{1 + \frac{W^2}{[h + (W-y) \tan \theta_1]^2}} \ .$$

Applying the binominal expansion to the square root,

$$(a + x)^n = a^n + na^{n-1} x + \frac{n(n-1)}{2!} a^{n-2} x^2 + \ldots \quad x^2 < a^2$$

we have

$$\sqrt{1 + \frac{W^2}{[\ ]^2}} = 1 + \frac{1}{2} \frac{W^2}{[h + (W-y) \tan \theta_1]^2} - \frac{1}{8} \frac{W^4}{[\ ]^4}$$

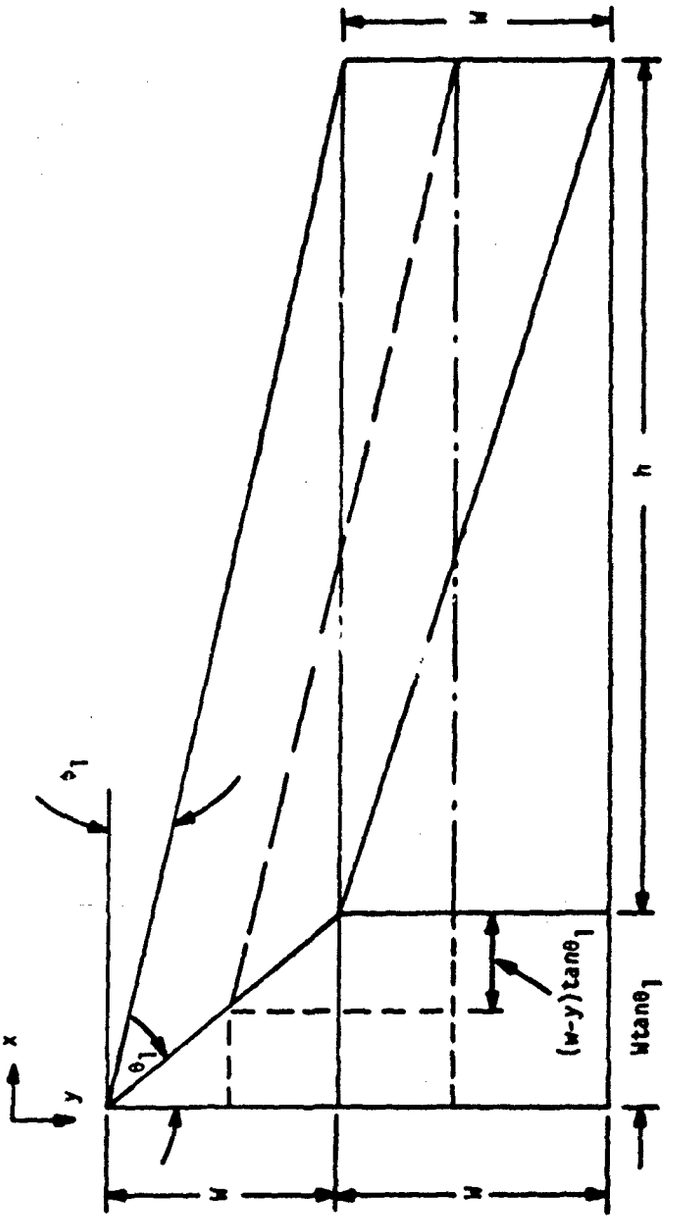

Figure 17. Diagram of Light Paths from Central and First Facet from Lens

Thus,

$$\Delta = (n-1)(W-y)\tan\theta_1 - \frac{W^2}{2[h + (W-y)\tan\theta_1]} - \frac{1}{8}\frac{W^4}{[\ ]^3}$$

From Equations 4 and 5 we have $\tan\theta_1 = \dfrac{W}{h[n\sqrt{1 + (\frac{W}{h})^2} - 1]}$

In the previous values, the largest $W/h = 0.0333$ so that $(W/h)^2 = 0.0011$, thus we can say to a very good approximation $\tan\theta_1 = \dfrac{W}{h[n-1]}$

Keeping only the first two terms in Δ we have

$$\Delta = \frac{(W-y)W}{h} - \frac{W^2}{2h[1 + \frac{(W-y)W}{(n-1)h}]}$$

The largest value of $\dfrac{(W-y)W}{(n-1)\,h^2}$ occurs when $y = 0$ or about 0.0044, thus this term can be dropped when compared with one to a very good approximation.

$$\Delta = \frac{(W-y)W}{h} - \frac{W^2}{2h} = \frac{W^2}{2h} - \frac{yW}{h}$$

When $y = 0$, $\Delta = W^2/2h$. When $y = -W$, $\Delta = -W^2/2h$ which agrees with direct evaluation at these two extremes.

At positions y_1 and y_2, we have $\Delta_1 - \Delta_2 = \dfrac{(y_2-y_1)}{h} W$

Following the description of Young's double slit experiment (References 27, 28) we see that the resultant intensity distribution maxima occurs at separations of $\Delta_1 - \Delta_2 = \lambda$. Therefore, for the separation of adjacent maxima $\Delta y = \dfrac{\lambda h}{W}$.

Using $W = 0.5$ cm, $\lambda = 0.532$ μm, $n = 1.460$, $h_1 = 21.7 - 1.3 = 20.4$ cm + 0.44 due to second lens 20.84 cm and $h_2 = 16.4 - 1.4 = 15.0$ cm. For the "20 cm" lens,

$$\Delta y = 0.532\ \mu m\ \frac{20.84\ cm}{0.5\ cm} = 22.17\ \mu m.$$

For the "15 cm" lens, $y = 15.96$ μm.

The ratio of these is 1.389. The experimentally measured values for the longer focal length lens of 20.65, 19.36, and 20.60 average out to 20.37 μm; for the shorter focal length lens, of 16.13, 15.36, and 15.58 average out to 15.69 μm. The ratio is 1.298. Thus, the experimental and calculated spacings due to the shorter lens agree to within 1.7%; for the longer lens, 8.8%. The ratios agree to within 7.0%.

In retrospect, it is not too surprising that there were interference effects between adjacent facets. The amazing thing is that the patterns from all the possible interactions seem to fall on top of each other. One would have expected to see a series of interpenetrating spot patterns which, hopefully, would cover most of the surface area. In the design of another faceted lens, perhaps one should deliberately introduce a slight variation in the location of focal strips or a slight difference in the focus of ± m facets.

SECTION IV

SUMMARY AND CONCLUSIONS

We have designed and fabricated a refractive laser beam homogenizer for use with a Nd:YAG laser at its fundamental (1.06 μm) and doubled (532 nm) frequencies. The system consists of a 2X beam expander and two faceted cylindrical lens with differing focal lengths. Each lens focusses its input into a strip the width of a facet. By orienting their axes at 90° angles and focussing them on the same plane, the beam is concentrated into a square focus 5mm on a side. This system takes an input beam with pronounced diffraction rings and produces a concentrated output which appears uniform to the eye. A 93% throughput of the beam expander and homogenizer system was measured at 532 nm. Subsequent experiments at the damage threshold of a silicon wafer, revealed that this apparent uniform focal spot when viewed under a microscope really consists of a rectangular array of hot spots with separations of 15.6 μm and 20.6 μm using 532 nm light. Due to the long coherence length of the Nd:YAG laser theoretically the light through the facets can be treated in a manner similar to Young's double fringe experiment. The output of each lens creates a pattern of linear fringes. The intersection of the two perpendicular patterns results in the observed array of hot spots. Calculations yield spacings of 15.96 μm and 22.17 μm. Thus, to be useful in laser melting and recrystallization, one must work in a region well above threshold or introduce further scrambling devices.

SECTION V

RECOMMENDATIONS

While we have demonstrated that this is an efficient means of scrambling a laser beam, further scrambling is necessary to make it useful for laser annealing semiconductor surfaces. Thus using it in conjunction with one of the other scrambling techniques mentioned in the introduction should result in a useful system.

There has been some discussion as to what is the appropriate orientation of the facets - toward or away from the incoming beam. To the eye there seemed to be no difference whether the flat faces of the faceted lenses were toward or away from the beam or a combination. General wisdom has it that for a sharper focus one generally wishes to have the curved (faceted) surfaces nearer the image. However, in higher power laser system there is another consideration to take into account. In laser damage studies of transparent materials, workers noticed that almost always damage was initiated at the exit face of the sample. A number of workers (References 29-33) have developed theories to explain this fact. Consequently, it would seem that from a practical viewpoint it would be desirable to have the flat faces away from the incoming beam. Thus if a damage spot occurred, it would be easier to grind down, repolish, and recoat the AR coating on the flat faces than to repair the faceted side.

REFERENCES

1. John F. Ready, Effects of High-Power Laser Radiation (Academic Press, NY, 1971) Pg 13-17.

2. Zhou Guosheng, P. M. Fauchet and A. E. Siegman, "Growth of Spontaneous Periodic Structures on Solids During Laser Illumination." Phys. Rev. B26 5366-5381 (1982) and references therein.

3. J. E. Sipe, Jeff F. Young, J. S. Preston and H. M. Van Driel and J. E. Sipe, "Laser-Induced Periodic Surface Structure. I. Theory," Phys. Rev. B27, 1141-1154 (1983). Jeff F. Young, J. S. Preston, H. M. Van Driel and J. E. Sipe, "LIPSS: II Experiments on Ge, Si, Al, and Brass." Phys. Rev B27 1155-1172 (1983) and references therein.

4. W. W. Simmons, D. R. Speck and J. T. Hunt, "Argus Laser System: Performance Summary," Applied Optics 17 999-1005 (1978).

5. J. W. Ogland, "Mirror System for Uniform Beam Transformation in High Power Annular Lasers," Applied Optics 17 2917-2923 (1978).

6. D. N. Mansell and T. T. Saito, "Design and Fabrication of a Nonlinear Waxicon," Optical Engineering 16 355-359 (1977).

7. P. W. Scott and W. H. Southwell, "Reflective Optics for Irradiance Redistribution of Laser Beams: Design," Applied Optics 20 1606-1610 (1981).

8. SPAWR Optical Research, Inc., 1527 Pomona Road, Corona, CA 91720, Data sheet 512.

9. R. E. Grojean, D. Feldman and J. F. Roach, "Production of Flat Top Beam Profiles for High Energy Lasers," Rev. Sci. Instrum. 51 375-6 (1980).

10. M. M. Chen, J. B. Berkowitz - Mattuck and P. E. Glaser, "The Use of a Kaleidoscope to Obtain Uniform Flux Over a Large Area in a Solar or Arc Imaging Furnace," Applied Optics 2 265-271 (1963).

11. K. Iwasaki, Y. Ohyama and Y. Nanaumi, "Flattening Laser Beam Intensity Distribution," Lasers and Applications 2(4), 76 (April 1983).

12. A. G. Cullis, H. C. Webber and P. Bailey, "A Device for Laser Beam Diffusion and Homogenization," J. Phys F: 12 688-689 (1979).

13. V. N. Alexseev, A. N. Zhilin, A. D. Starikov, and V. N. Chernov, "Formation of a Spatial Profile of a Beam in a Laser Amplifier by a System Comprising a Hard Aperture and a Spatial Filter," Sov. J. Quantum Electron. 10 1186-1188 (1980).

14. M. R. Latta and K. Jain, "Beam Intensity Uniformization by Mirror Folding," IBM Research Report RJ 3935 (44535) 6/24/83.

REFERENCES (Continued)

15. Kanti Jain, "Laser Applications in Semiconductor Microlithography," Lasers and Applications 2(9), 49-56 (Sept. 1983).

16. B. Roy Frieden, "Lossless Conversion of a Plane Laser Wave to a Plane Wave of Uniform Irradiance," Applied Optics 4 1400-1403 (1965).

17. Patrick W. Rhodes and David L. Shealy, "Refractive Optical Systems for Irradiance Redistribution of Collimated Radiation: Their Design and Analysis," Applied Optics 19 3545-3553 (1980).

18. Dean F. Cornwell, "Intensity Redistribution," J. Opt. Soc. Am. 69 1456 (1979).

19. Dean F. Cornwell, "Non-projective Transformations in Optics," SPIE 294 67-72 (1981).

20. T. E. Horton and J. H. McDermit, "Design of a Specular Aspheric Surface to Uniformly Radiate a Flat Surface Using a Nonuniform Collimated Radiation Source," Trans. ASME: J. Heat Transfer C94 453-458 (1972).

21. Thomas J. Magee and T. Keith McNab, "Laser Processing of Semiconductor Silicon: Part I," Solid State Technology 25(7) 74-82 (July, 1982); Part II 25(12) 101-105 (Dec., 1982).

22. Y. Belvaux and S. P. S. Virdi, "A Method for Obtaining a Uniform Non-Gaussian Laser Illumination," Optics Communications 15 193-195 (1975).

23. Wilfrid B. Veldkamp, "Laser Beam Profile Shaping with Binary Diffraction Gatings," Optics Communications 38 381-386 (1981).

24. W. B. Veldkamp and C. J. Kastner, "Beam Profile Shaping for Laser Radars That Use Detector Arrays," Appl. Optics 21 345-346 (1982).

25. W. B. Veldkamp, "Laser Beam Profile Shaping with Interlaced Binary Diffraction Gratings," Appl. Optics 21 3209-3212 (1982).

26. W. B. Veldkamp, "Technique for Generating Focal-Plane Flattop Laser-Beam Profiles," Rev. Sci. Instrum 53 294-297 (1982).

27. Francis A. Jenkins and Harvey E. White, "Fundamentals of Optics", 2nd ed (McGraw Hill, NY, 1950) Chapters 13, 16, 17.

28. Donald C. O'Shea, W. Russell Callen, and William T. Rhodes, "Introduction to Lasers and Their Applications," (Addison-Wesley, Reading MA, 1977) pp. 23-28.

29. M. D. Crisp, N. L. Boling, and G. Dube, "Importance of Fresnel Reflections in Laser Surface Damage of Transparent Materials," Appl. Phys Lett. 21 364 (1972).

REFERENCES (Concluded)

30. N. L. Boling, M. D. Crisp, and G. Dube. "Laser Induced Surface Damage," Appl. Optics 12 650 (1973).

31. M. D. Crisp, "Laser-Induced Surface Damage of Transparent Dielectrics," IEEE J. Quantum Electronics QE-10 57 (1974).

32. P. A. Miles, "Static Profile Calorimetry of Laser Materials," Appl. Optics 16, 2897 (1977).

33. Joseph A. Apfel, private communication.

U.S. Government Printing Office 1984 559 065/10502